ELSEVIER

Contents lists available at ScienceDirect

Acta Biomaterialia

journal homepage: www.elsevier.com/locate/actbio



Full length article

High oxygen preservation hydrogels to augment cell survival under hypoxic condition



Hong Niu^{a,b}, Chao Li^a, Ya Guan^{a,b}, Yu Dang^{a,b}, Xiaofei Li^a, Zhaobo Fan^a, Jie Shen^c, Liang Ma^d, Jianjun Guan^{a,b,*}

- ^a Department of Materials Science and Engineering, The Ohio State University, Columbus, OH 43210, USA
- ^b Department of Mechanical Engineering and Materials Science, Washington University in St. Louis, St. Louis, MO 63130, USA
- ^c Orthopaedic Surgery, Washington University School of Medicine, St. Louis, MO, 631310, USA
- ^d Division of Dermatology, Washington University School of Medicine, St. Louis, MO, 631310, USA

ARTICLE INFO

Article history: Received 23 October 2019 Revised 18 December 2019 Accepted 13 January 2020 Available online 15 January 2020

Keywords:
Thermosensitive hydrogel
Oxygen preservation
Stem cell transplantation
Cell survival
Ischemic tissue

ABSTRACT

Cell therapy is a promising approach for ischemic tissue regeneration. However, high death rate of delivered cells under low oxygen condition, and poor cell retention in tissues largely limit the therapeutic efficacy. Using cell carriers with high oxygen preservation has potential to improve cell survival. To increase cell retention, cell carriers that can quickly solidify at 37 °C so as to efficiently immobilize the carriers and cells in the tissues are necessary. Yet there lacks cell carriers with these combined properties. In this work, we have developed a family of high oxygen preservation and fast gelation hydrogels based on N-isopropylacrylamide (NIPAAm) copolymers. The hydrogels were synthesized by reversible addition-fragmentation chain transfer (RAFT) polymerization of NIPAAm, acrylate-oligolactide (AOLA), 2hydroxyethyl methacrylate (HEMA), and methacrylate-poly(ethylene glycol)-perfluorooctane (MAPEGPFC). The hydrogel solutions exhibited sol-gel temperatures around room temperature and were flowable and injectable at 4°C. They can quickly solidify (≤ 6 s) at 37°C to form flexible gels. These hydrogels lost 9.4~29.4% of their mass after incubation in Dulbecco's Phosphate-Buffered Saline (DPBS) for 4 weeks. The hydrogels exhibited a greater oxygen partial pressure than DPBS after being transferred from a 21% O2 condition to a 1% O2 condition. When bone marrow mesenchymal stem cells (MSCs) were encapsulated in the hydrogels and cultured under 1% O2, the cells survived and proliferated during the 14-day culture period. In contrast, the cells experienced extensive death in the control hydrogel that had low oxygen preservation capability. The hydrogels possessed excellent biocompatibility. The final degradation products did not provoke cell death even when the concentration was as high as 15 mg/ml, and the hydrogel implantation did not induce substantial inflammation. These hydrogels are promising as cell carriers for cell transplantation into ischemic tissues.

Statement of Significance

Stem cell therapy for ischemic tissues experiences low therapeutic efficacy largely due to poor cell survival under low oxygen condition. Using cell carriers with high oxygen preservation capability has potential to improve cell survival. In this work, we have developed a family of hydrogels with this property. These hydrogels promoted the encapsulated stem cell survival and growth under low oxygen condition.

 $\ensuremath{\mathbb{C}}$ 2020 Acta Materialia Inc. Published by Elsevier Ltd. All rights reserved.

1. Introduction

Cell therapy has been considered as a promising strategy for ischemic tissue regeneration, yet experiences low therapeutic efficacy [1], largely due to poor cell survival under the low oxygen condition of the ischemic tissues [2,3]. Therefore, supply of oxygen to the transplanted cells is of importance to increase cell survival.

^{*} Corresponding author at: Department of Mechanical Engineering and Materials Science, Washington University in St. Louis, 303F Jubel Hall (Office), 340 Whitaker Hall (Lab), Campus Box 1185, St. Louis, MO 63130, USA.

E-mail address: jguan22@wustl.edu (J. Guan).

Quick vascularization of ischemic tissues represents an effective and long-term strategy to supply oxygen to improve cell survival [4,5], yet a large percent of cells die before vascularization is established [6–8]. Direct provision of oxygen upon cell transplantation has been demonstrated to improve cell survival [9,10]. The approaches that have been used to supply oxygen include hyperbaric oxygenation (HBO) [11–13], in situ generation of oxygen in tissues [14,15], and oxygen carriers [16–18].

HBO is a systemic oxygen delivery approach that has been used to increase tissue oxygen level. HBO therapy has been shown to stimulate the survival of colonic stem cell, neural stem cell, and mesenchymal stem cell in ischemic tissues [19–22]. While HBO therapy is convenient, there are disadvantages associated with it especially for ischemic tissue repair/regeneration. First, this systemic oxygen delivery approach cannot efficiently diffuse oxygen by blood to the ischemic area that is poorly vascularized. Second, HBO therapy cannot provide oxygen to ischemic tissues in a sustainable manner. The oxygen level decreases quickly after the therapy. Third, HBO therapy increases oxygen level in healthy tissues. This may increase tissue oxidative stress leading to adverse effects [23].

In situ generation of oxygen in the ischemic tissues is an approach that can locally and directly deliver oxygen to the transplanted and host cells. MgO₂ [24], CaO₂ [25-27] and H₂O₂ [28,29] have been used as source of oxygen. MgO2 and CaO2 react with water to form H_2O_2 followed by H_2O_2 decomposition to form molecular oxygen. Encapsulation of MgO2, CaO2, and H2O2 into polymers or microspheres allowed oxygen release to last for several hours to 2 weeks. The released oxygen promoted cell survival in the ischemic skin [30]. One of the concerns for peroxide-based oxygen release is that H2O2 may be toxic to cells if it is not converted quickly into molecular oxygen [31]. To avoid direct contact of cells with H₂O₂, catalase was added to the polymers to timely convert the released H_2O_2 into oxygen [32,33]. Studies have shown that this approach largely improved the survival of cardiosphere derived cell under low oxygen condition in vitro [34], and cardiac cell survival in vivo [9,35]. Nevertheless, the increased oxidative stress due to burst release needs to be minimized for in vivo applications and clinical uses.

Using oxygen carriers to deliver oxygen into ischemic tissues has proven to be efficient in animal models and clinical trials [36,37]. Hemoglobin [38,39] and fluorinated compounds [40-42] are typical oxygen carriers. Utilization of hemoglobin to supply oxygen to MSCs significantly promoted cell survival and growth under hypoxic conditions [43,44]. One of the major challenges to the clinical use of hemoglobin is its instantaneous oxygen release. In addition, hemoglobin generates reactive oxygen species (ROS) after the initial oxygen release [45,46]. Compared to the above mentioned oxygen-generating species, peroxide-based releasing biomaterials and hemoglobin-based oxygen carriers, perfluorocarbons (PFCs) have potential to overcome these disadvantages. PFCs are a type of oxygen carrier with high oxygen solubility (20-fold higher than water) [47,48]. This remarkable oxygen carrying property allows PFCs to be used in artificial blood [49]. PFCs have also been applied during tissue culture to increase the survival of MSCs and adipose-derived stem cells under hypoxic conditions [50,51]. However, PFCs have a short in vivo retention time due to their low molecular weight [52], which limits their applications in ischemic tissue regeneration. Conjugation of PFCs into biomaterials may increase their retention time, and hence short-term cell survival [17]. Yet current reports provide limited evidence that using PFC-conjugated biomaterials improves long-term cell survival under hypoxic conditions [53].

The objective of this study was to develop a family of PFC-conjugated hydrogels with increased oxygen partial pressure, so as to augment cell survival under hypoxic conditions. These hydrogels

are also fast gelling and thermosensitive. Fast gelation enables the hydrogels to quickly solidify so as to immobilize cells in the tissues and increase cell retention. [54–58] Thermosensitivity allows the hydrogels to be solidified at body temperature yet flowable at temperatures below thermal transition temperature. These attractive properties make the developed hydrogels more suitable for cell therapy than the oxygen delivery biomaterials without these properties. In this work, we characterize the chemical and physical properties and the *in vitro* and *in vivo* biocompatibility of the hydrogels, and we test their ability to improve MSC survival under low oxygen conditions.

2. Experimental section

2.1. Materials

All materials were purchased from Sigma-Aldrich, unless otherwise stated. Perfluorooctanoyl chloride glycol) methacrylate poly(ethylene (PEGMA), Aesar), (dodecylthiocarbonothioylthio)-2-methylpropionic acid (DDMAT), triethylamine (TEA, Fisher-Scientific), D, L-lactide, acryloyl chloride, lithium phthalocyanine (Alfa Aesar), and 2, 2'-azobis (2methylpropionitrile) (AIBN) were used as received. NIPAAm (TCI) was recrystallized three times using ethyl acetate and hexane. HEMA (Alfa Aesar) was used after removing polymerization inhibitors using a packed-bed column filled with inhibitor remover. Acrylate oligolactide (AOLA) was synthesized by acrylation of oligolactide (HO-OLA-OCH3) with acryloyl chloride, as described in our previous reports [9,59,60].

2.2. Synthesis of PFC containing macromer

PFC-containing macromer MAPEGPFC was synthesized by the reaction of perfluorooctanoyl chloride with MAPEG (Scheme 1). In brief, MAPEG (12.1 g, 23.0 mmol) and dichloromethane (DCM, 50 mL) were added to a 250 mL three-neck flask equipped with a dropping funnel and a magnetic stirrer. After the solution was purged with N₂ for 15 min, TEA (3.53 g, 35.0 mmol) was added. The solution was then cooled in an ice bath. A solution of perfluorooctanoyl chloride (5.73 mL, 23.0 mmol) in DCM (20 mL) was added dropwise for 1 h. The mixture was stirred overnight in an ice bath, then after filtration, the solution was concentrated by a rotary evaporator and dissolved in ethyl acetate (100 mL). The solution was washed sequentially with saturated sodium bicarbonate and saturated sodium chloride aqueous solutions, which were removed after washing by phase separation. The organic phase was dried over sodium sulfate and then concentrated under vacuum. The obtained product, a yellow oil, had a yield of ~70%. Its structure was confirmed by ¹H NMR (400 MHz, CDCl₃) and ¹⁹F-NMR (400 MHz, CDCl₃) spectra.

2.3. Synthesis of hydrogels

Hydrogel polymers poly(NIPAAm-co-HEMA-co-AOLA-co-MAPEGPFC) and poly (NIPAAm-co-HEMA-co-AOLA-co-MAPEG), were synthesized by reversible addition-fragmentation chaintransfer (RAFT) polymerization, using AIBN as an initiator and DDMAT as the chain transfer agent (CTA) (Scheme 2). In a typical polymerization procedure, the monomers (NIPAAm, HEMA, AOLA, and MAPEGPFC or MAPEG) were dissolved in dimethylformamide (DMF) with molar ratios of 77/10/8/5 and 72/10/8/10, respectively (Table 1). The solution concentration was controlled at 10%. It was then added into a 250 mL three-necked flask. After flushing with N₂ for 15 min, a degassed solution of AIBN and CTA in DMF was injected into the flask. The molar ratio of the comonomers, CTA and AIBN, was 100/1/0.2. The reaction was conducted at

MAPEG PFC MAPEGPFC

Scheme 1. Synthesis of macromer MAPEGPFC by reaction of pentadecafluorooctanoyl chloride with poly(ethylene glycol) methacrylate.

Scheme 2. Synthesis and degradation of poly (NIPAAm-co-HEMA-co-AOLA-co-MAPEGPFC) and poly (NIPAAmco-HEMA-co-AOLA-co-MAPEG) by RAFT polymerization.

 Table 1

 Monomer feed ratio, and polymer composition and molecular weight.

| Hydrogel | Composition | Feed ratio | Actual ratio ^a | M _n | M_{w} | PDI |
|---|--|---------------------------------------|---|--|--|----------------------|
| PNHAM-PFC0 PNHAM-PFC5 PNHAM-PFC10 | NIPAAm/HEMA/AOLA/PEGMA NIPAAm/HEMA/AOLA/PEGMAPFC NIPAAm/HEMA/AOLA/PEGMAPFC | 72/10/8/10 77/10/8/5 72/10/8/10 | 72.3/9.4/8.6/9.7 76.2/9.4/8.8/5.6 71.5/10.5/8.2/9.8 | $\begin{array}{c} 2.9 \ \times \ 10^4 \\ 2.5 \ \times \ 10^4 \\ 2.6 \ \times \ 10^4 \end{array}$ | $\begin{array}{c} 5.0 \ \times \ 10^4 \\ 3.9 \ \times \ 10^4 \\ 3.8 \ \times \ 10^4 \end{array}$ | 1.72 1.56 1.46 |

^a Calculated from ¹H NMR.

65 °C for 20 h. After cooling to room temperature, the polymer was precipitated in diethyl ether, and further purified by tetrahydrofuran/diethyl ether twice. The yield was ~60%. The structure was confirmed by ¹H NMR spectra (400 MHz, CDCl₃), and the composition was calculated based on the spectra. The molecular weight of polymers were measured with an analytical gel permeation chromatography (GPC) equipped with light scattering and refractive index detectors (Wyatt Tech). DMF was used as a solvent. The hydrogels without PFC, and with 5% and 10% PFC, were abbreviated as PNHAM-PFC0, PNHAM-PFC5, and PNHAM-PFC10, respectively.

2.4. Characterization of oxygen partial pressure in hydrogels

To test oxygen preservation capability of the hydrogels, the oxygen partial pressure (pO₂) in the hydrogels at 21% and 1% O₂ conditions were measured using electron paramagnetic resonance (EPR). Oxygen sensitive lithium phthalocyanine (LiPc) was used as EPR probe [61]. LiPc particles (<1 μ m in diameter, 40 mg/mL in DPBS) were thoroughly mixed with 8% hydrogel solution that was stirred under atmospheric condition (21% O₂) overnight. 200 μ L of the mixture was transferred to a 37 °C water bath for gelation. After 30 min, the solid gel was loaded into a gas permeable EPR tube under atmospheric condition (21% O₂). The EPR spectrum was recorded on an X-band EPR instrument (Bruker). The parameters used included 0.1 mW for microwave power, 9.8 GHz for frequency and 1.0 dB for attenuation. After measurement under 21% O₂, the

sample was flushed with $1\% O_2$ to reach equilibrium as monitored by EPR. The EPR spectrum was then recorded. LiPc loaded with DPBS was used as control. pO_2 was calculated based on linewidth of the sample and calibration curve of linewidth vs. oxygen concentration. Four replicates for each hydrogel type were tested.

2.5. Characterization of hydrogel properties

The polymers were dissolved in DPBS at 4 °C overnight to form 8% hydrogel solutions. Each hydrogel solution was pre-cooled to 4 °C and transferred into a 1 mL syringe. The injectability was then tested by injecting the solution through a 26 G needle. To determine thermal transition temperature of each hydrogel solution, differential scanning calorimetry (DSC) was used. The temperature range was -10 °C to 80 °C, and the heating rate was 10 °C/min. The thermal transition temperature was the temperature at the maximum endothermal peak [62]. Gelation time of hydrogel solution was measured by a temperature controllable Olympus microscope following our previously established protocol [59,63]. The time needed for a 4 °C solution to become completely opaque at 37 °C was defined as gelation time. To determine hydrogel water content, the 8% hydrogel solution was solidified at 37 °C. 200 µL of pre-warmed DPBS was then added. Following incubation at 37 °C for 5 h, samples (n = 4) were taken out and weighed. Water content was calculated as $(w_2-w_1)/w_1 \times 100\%$, where w_1 and w_2 were the mass of dry and wet hydrogels, respectively.

To characterize hydrogel mechanical properties, the 37 °C solid gels were cut into specimens of 5 mm \times 5 mm \times 25 mm. Each specimen was then loaded into an Instron tensile tester equipped with a 37 °C water bath. The testing was conducted using a crosshead speed of 50 mm/min, and a load cell of 44.5 N. Hydrogel Young's modulus was quantified from the stress-strain curve using a Matlab program [64].

To characterize hydrogel degradation property, 200 μ L of hydrogel solution (8%) was transferred into a 1.5 mL microcentrifuge tube, followed by incubation in a 37 °C water bath for solidification. 200 μ L of DPBS was then added. The tubes were placed in a 37 °C water bath. After 1, 2, 3, and 4 weeks of incubation, samples (n=4 for each hydrogel type at each time point) were collected, freeze-dried and weighed. Weight remaining was calculated.

To determine biocompatibility of the final degradation product, poly (NIPAAm-co-HEMA-co-AAc-co-MAPEGPFC) with feed ratio of 72/10/8/10 (NIPAAm/HEMA/AAc/MAPEGPFC) was synthesized by RAFT polymerization using the same approach as for the hydrogels. This polymer represents the final degradation product of PNHAM-PFC10. The polymer was dissolved in DPBS to obtain solutions with concentrations of 1, 5, 10, and 15 mg/mL, respectively. To test cytotoxicity of the final degradation product, rat cardiac fibroblasts were seeded in a 96-well tissue culture plate. The density was controlled at 2 \times 10⁵ cells/mL. The cells were cultured in DMEM supplemented with 10% FBS. After 24 h of culture, 50 μ L of the final degradation product solution was added to each well (n=4 for each concentration). The wells without addition of the final degradation product solution were used as control. Cell viability was determined by MTT assay following 48 h of culture [59].

2.6. MSC culture in the hydrogels

Rat bone marrow derived MSCs were used for encapsulation in the hydrogels to investigate cell survival and paracrine effects under normal and hypoxic conditions. The cells were cultured using α MEM supplemented with 10% FBS and 1% Penicillin/Streptomycin. Prior to encapsulation, the cells were stained with a live cell tracker CMFDA (Invitrogen) [59]. The labelled MSCs were suspended in the culture medium followed by mixing with the hydrogel solutions (8%) that were stirred under atmospheric condition (21% O₂) overnight. Based on our previous study [65], the final seeding density of 8 million/mL was used. The mixture was then transferred into 1.5 mL microcentrifugation tubes (200 µL/tube). The tubes were placed in a 37 °C incubator for gelation. After 30 min, 200 µL of culture medium was added into each tube. The cells were cultured under two oxygen conditions (21% and 1%) for 2 weeks, respectively. To determine MSC survival and proliferation in the hydrogels, double-stranded DNA (dsDNA) content was measured by PicoGreen dsDNA assay [59] after 1, 3, 7, and 14 days of culture (n = 4 for each condition at each time point). To visualize live cells, the samples collected at days 1, 3, 7 and 14 were imaged by a confocal microscope.

MSC paracrine effects were characterized by real-time RT-PCR. The expressions of PDGFB and IGF-1 were quantified. RNA extraction and cDNA synthesis were performed following our established protocols [59,64]. The primer sequences were listed in Table 2. Real-time RT-PCR was conducted with Maxima SYBR Green/Fluorescein master mix on an Applied Biosystem 7900 system. Housekeeping gene was β -actin. A standard $\triangle\triangle$ Ct method was utilized to quantify fold of increase [57,59].

2.7. In vitro oxygen tension within hydrogels

Oxygen tension in the hydrogels with or without MSC encapsulation was measured using an OxyliteTM oxygen monitor equipped with a fiber-optic oxygen micro-sensor (Oxford Optronix

Table 2Sequences of primers used for real-time RT-PCR.

| Gene | Primer Sequences | |
|----------------|--------------------------------------|--|
| β -actin | Forward: AAGATCAAGATCATTGCTCCTC | |
| | Reverse: GGACTCATCGTACTCCTG | |
| PDGFB | Forward: GATGCCTTGGAGACAAACCTGACA | |
| | Reverse: ATACTTCTCTTCCTCCTGCGAATGGGC | |
| IGF-1 | Forward: TGACATGCCCAAGACTCAGAAGGA | |
| | Reverse: GGTTGCTCAAGCAGCAAAGGATCT | |

Ltd, Britain). Before measurement, the oxygen sensor was calibrated under normal air (21% O_2), 15% O_2 , and 1% O_2 conditions to validate the accuracy. All three polymers, PNHAM-PFCO, PNHAM-PFC5 and PNHAM-PFC10, were separately dissolved in DPBS to form uniform hydrogel solutions. Each hydrogel solution (200 μL) was placed in a 1.5 mL microcentrifuge tube in a 37 °C incubator under 21% O₂ for 30 min to allow gelation. The sensor was then introduced into the hydrogel to measure oxygen partial pressure. For each sample, 7 measurements were made at 7 different locations of the bulk of the hydrogel. For each measurement, the oxygen tension was recorded when a stable reading on the monitor was established (it took ≤10 min). Four samples for each hydrogel type were tested. Following the measurements, a hole was punched on the lid of each microcentrifuge tube with an 18 G needle. The tube was placed in a hypoxic incubator with 1% O2. The oxygen tension was tested after incubation for 8, 72, 120 and 168 h, respectively. For each sample at each time point, oxygen tension at 7 different locations of the bulk was measured. The above method was applied for testing oxygen tension in hydrogels encapsulated with MSCs.

2.8. Subcutaneous injection of hydrogels into mice

All animal experiments were conducted in accordance with the National Institutes of Health Guide for handling laboratory animals and the animal protocol was approved by the Institutional Animal Care and Use Committee of the Ohio State University. C57BL/6 mice aged 9 weeks were used. The 8% hydrogel solutions were cooled in an ice bath and sterilized under UV light for 30 min. The hydrogel solution was injected subcutaneously into mice (50 μ L/injection, 2 injection/mouse, 3 mice for each hydrogel type). Mice injected with type I rat tail collagen gel (3–4 mg/ml, Corning) were used as controls. After 4 weeks of implantation, the samples were collected, fixed in 4% paraformaldehyde, and sectioned into 5 μ mthick slices. The sections were stained using F4/80 antibody [66], and the ratio of F4/80 positive cells was quantified from confocal images (n=8) [59].

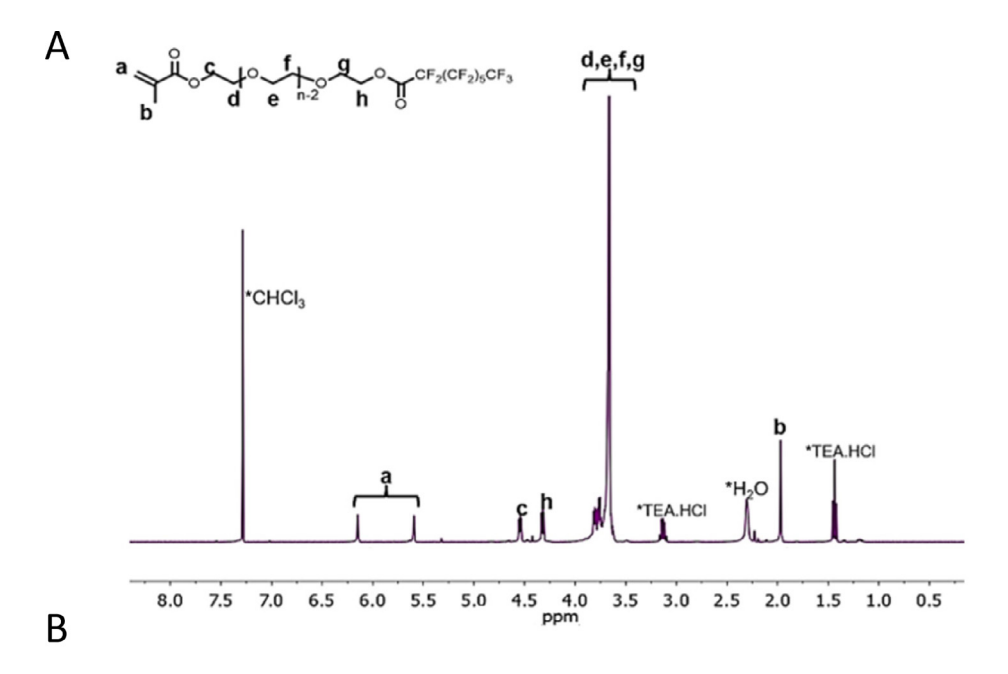
2.9. Statistical analysis

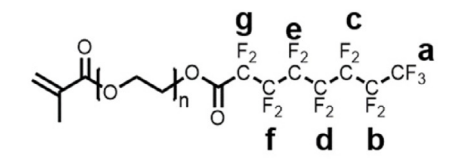
Data were reported as mean \pm standard deviation. Data analysis was performed using one-way ANOVA with post hoc Neuman – Keuls testing. Statistical significance was defined as p < 0.05.

3. Results

3.1. Synthesis of macromer and hydrogel polymers

The macromer MAPEGPFC was synthesized by the reaction of MAPEG with perfluorooctanoyl chloride. In the 1H NMR spectrum (Fig. 1A), all characteristic peaks for protons in PEGMA were appeared [C \underline{H}_2 = (a), -C \underline{H}_3 (b), -C(=0)OC \underline{H}_2 - (c), -OC \underline{H}_2 - (d, e, f, g), and -CH₂-C \underline{H}_2 -O-C(=0)- (h)]. In the 19 F-NMR spectrum (Fig. 1B), the characteristic peaks for fluorine in CF₃ (a) and CF₂ (b-f) were observed. The three hydrogel polymers based on NIPAAm, HEMA, AOLA, and MAPEGPFC or MAPEG were synthesized by RAFT





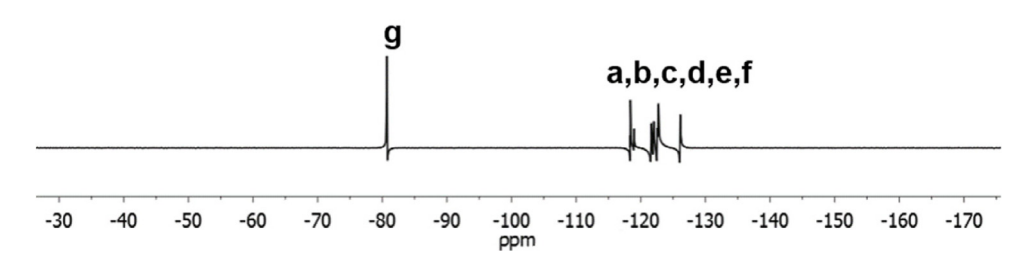


Fig. 1. ¹H-NMR spectrum (A) and ¹⁹F-NMR spectrum (B) of the synthesized monomer MAPEGPFC. CDCl₃ was used as a solvent.

polymerization. Free radical polymerization using AIBN as an initiator cannot effectively polymerize the monomers. A typical $^1\mathrm{H}$ NMR spectrum exhibited the characteristic proton peaks of each monomer unit [NIPAAm (a and b), HEMA (c and d), AOLA (e) and PEGMAPFC (f and g)] (Fig. 2). The hydrogel composition was calculated based on the $^1\mathrm{H}$ NMR spectra. All three polymers possessed ratios of all four monomers consistent with the initial feed ratios (Table 1). The number average molecular weights of the synthesized polymers ranged from 2.5 to 2.9 \times 10 4 g/mol, and weight molecular weights were in the range of 3.8 - 5.0 \times 10 4 g/mol.

3.2. Oxygen preservation property of the hydrogels

To investigate oxygen preservation property of the hydrogels when transferring the samples from the 21% $\rm O_2$ condition to the 1% $\rm O_2$ condition, $\rm pO_2$ in the hydrogels was measured under both conditions using EPR. Under 21% $\rm O_2$, the hydrogel without PFC (PNHAM-PFC0) had a $\rm pO_2$ significantly lower than that of DPBS (p < 0.05, Table 3). Introducing 5% PFC into the hydrogel (PNHAM-PFC5) significantly improved the $\rm pO_2$ similar to that of DPBS (p < 0.01 PNHAM-PFC5 vs. PNHAM-PFC0; p > 0.05 PNHAM-PFC5

Table 3 Oxygen partial pressure pO_2 tested for DPBS, PNHAM-PFC0, PNHAM-PFC5, and PNHAM-PFC10 under normal (21% O_2) and hypoxia (1% O_2) conditions. pO2 was calculated based on the calibration curve obtained for oxygen content and line width change in EPR spectrums.

| Group | pO ₂ under 21% O ₂ (mm Hg) | pO ₂ under 1% O ₂ (mm Hg) |
|---|---|--|
| DPBS PNHAM-PFC0 PNHAM-PFC5 PNHAM-PFC10 | 134.3 ± 15.2 101.7 ± 8.4 133.6 ± 9.8 138.4 ± 10.7 | 35.0 ± 3.1 28.1 ± 2.9 62.3 ± 5.7 75.8 ± 8.2 |

vs. DPBS). Further increase of PFC to 10% (PNHAM-PFC10) substantially increased the pO $_2$ (p>0.05 PNHAM-PFC5 vs. PNHAM-PFC10). Under 1% O $_2$ condition, the pO $_2$ in all 3 hydrogels were dropped. Yet the PNHAM-PFC5 and PNHAM-PFC10 had remarkably greater pO $_2$ than the PNHAM-PFC0 (p<0.01 PNHAM-PFC5 and PNHAM-PFC10 exhibited significantly higher pO2 than PNHAM-PFC5 (p<0.05). These results demonstrate that the developed PFC-containing hydrogels had good oxygen preservation property.

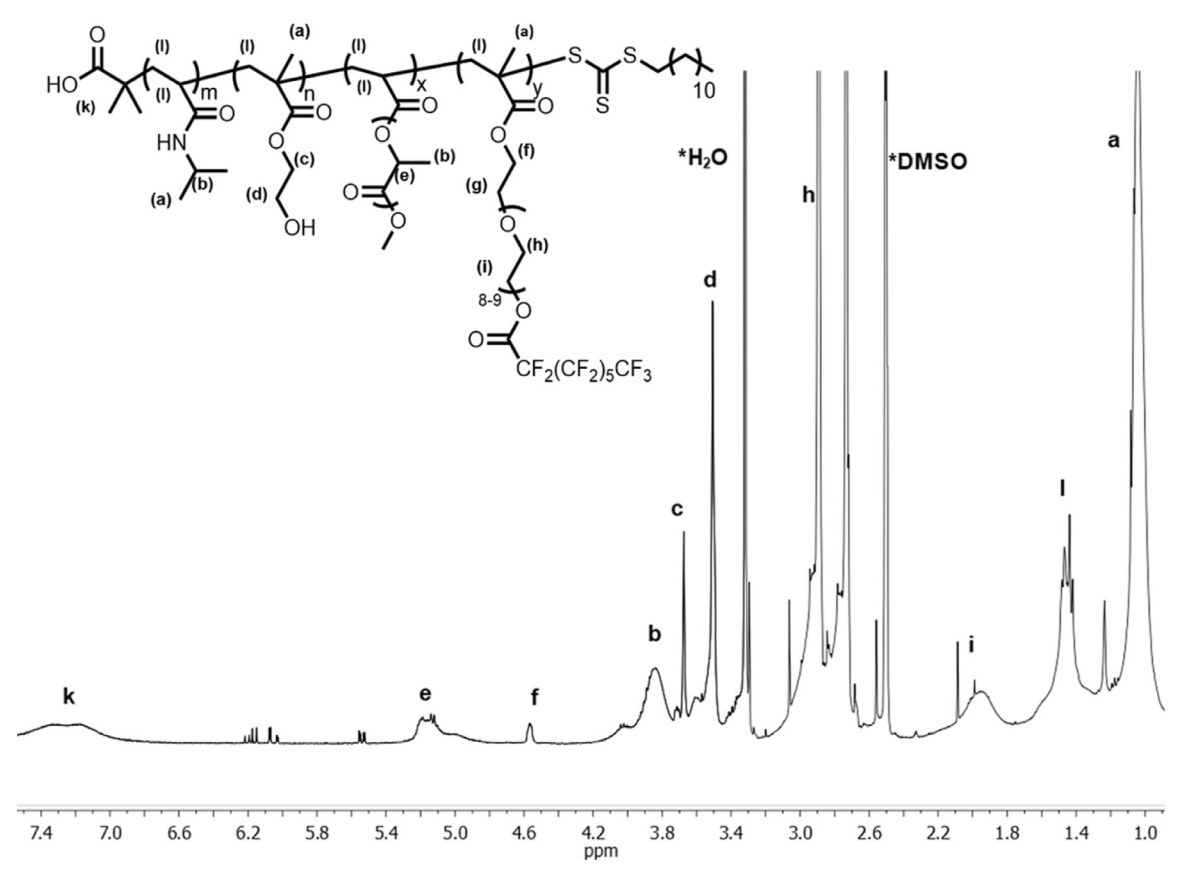


Fig. 2. ¹H-NMR spectrum of hydrogel PNHAM-PFC10. DMSO-d₆ was used as solvent.

Table 4Injectability, water content, thermal transition temperature, and Young's modulus of hydrogel PNHAM-PFC5 and PNHAM-PFC10.

| Hydrogel | Injectability | | Thermal transition temperature (°C) | Young's Modulus (kPa) |
|---------------------------|---------------|------------------|--------------------------------------|--------------------------|
| PNHAM-PFC5 PNHAM-PFC10 | +++ | $67\pm2\\84\pm3$ | 23 ± 1 29 ± 2 | 18 ± 3 12 ± 3 |

3.3. Injectability, thermal transition temperature, water content, and mechanical properties of the hydrogels

The hydrogels PNHAM-PFC5 and PNHAM-PFC10, which had better oxygen preservation capability were selected for physical property characterization. Both hydrogel solutions (4 °C, 8%) can be readily injected through a 26 G needle commonly used for tissue injection (Fig. 3A). The 4 °C hydrogel solutions were solidified within 6 s at 37 °C. The thermal transition temperatures of the hydrogel solutions were measured by DSC (Table 4). Both hydrogel solutions had thermal transition temperatures well below 37 °C, suggesting that they can solidify at 37 °C. The hydrogel PNHAM-PFC10 exhibited a higher thermal transition temperature than PNHAM-PFCC5. Water content of the hydrogels was dependent on their compositions. The increase of MAPEGPFC content from 5% to 10% significantly augmented water content from 66.5% to 84.3% (p<0.05. Table 4).

The hydrogels were highly flexible as they were stretchable at 37 °C (Figs. 3D and E, and 4). Both hydrogels had breaking strains higher than 100% (the first 100% of strain was shown in Fig. 4 to better demonstrate the initial difference in mechanical behaviors of the two hydrogels). Young's modulus of the hydrogel with 5% MAPEGPFC was 18 \pm 3 kPa. It was significantly decreased

to 12 \pm 3 kPa when the MAPEGPFC content was increased to 10% (p < 0.05. Table 4).

3.4. Hydrogel degradation and cytotoxicity of the degradation product

Hydrogels PNHAM-PFC5 and PNHAM-PFC10 gradually lost weight during the incubation in 37 °C DPBS for 4 weeks. PNHAM-PFC5 exhibited a relatively slow and linear weight loss profile, while PNHAM-PFC10 lost weight quicker than PNHAM-PFC5 in the period of week 2 and week 4 (Fig. 5A). At day 28, PNHAM-PFC10 had a significantly higher weight loss than PNHAM-PFC5 (p < 0.05). The final degradation products include lactic acid and high molecular weight polymer II in Scheme 2. It is known that lactic acid is nontoxic. To evaluate cytotoxicity of the high molecular weight polymer II, the final degradation product of PNHAM-PFC10 was synthesized. Rat cardiac fibroblasts were used to test cytotoxicity. Based on the structure change before and after degradation, the concentration of degradation products was estimated less than 15 mg/mL [59]. Cell viability did not significantly decrease even when the final degradation product concentration was as high as 15 mg/mL (Fig. 5B). These results demonstrate that the degradation products are nontoxic.

3.5. MSCs proliferation and paracrine effects in hydrogels under normal and hypoxic conditions

To evaluate cell proliferation in the developed hydrogels under normal oxygen condition, MSCs were encapsulated in the hydrogels and cultured for 14 days. Fig. 6A demonstrates that MSCs were able to proliferate in the hydrogels as cell dsDNA content was increased. The more pronounced proliferation was found for

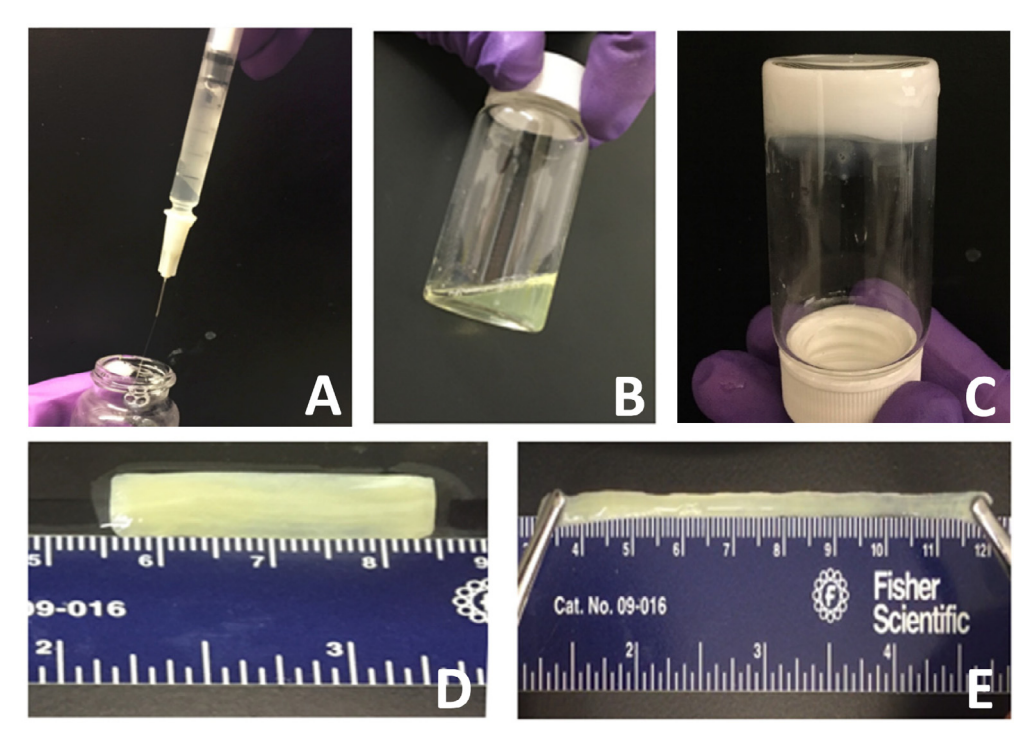


Fig. 3. Flowability, injectability, gelation, and stretchability of PNHAM-PFC hydrogel. (A) 4 °C solution was injectable through a 26-gage needle; (B) hydrogel solution was flowable at 4 °C; (C) hydrogel solution formed solid gel at 37 °C; (D) solid gel before stretching at 37 °C; and (E) solid gel after stretching at 37 °C.

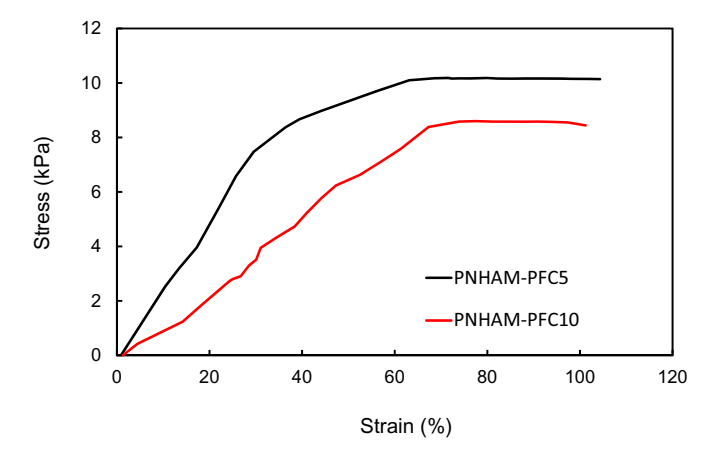


Fig. 4. Tensile stress-strain curves of PNHAM-PFC hydrogels. PNHAM-PFC5 and PNHAM-PFC10 represent hydrogels with PFC content of 5% and 10%, respectively.

the hydrogel PNHAM-PFC10 that had the highest content of PFC (Fig. 6A). At day 14, its dsDNA content was increased for more than 3 times compared to that at day 1 (p < 0.01). The dsDNA content was also significantly greater than that in the PNHAM-PFC5 and PNHAM-PFC0 groups (p < 0.05). Live cell imaging results (Fig. 6E) were consistent with dsDNA data, demonstrating that PFC-containing hydrogels can promote cell growth.

To determine whether the oxygen preservation hydrogels can promote MSC survival under hypoxic condition, the cells were encapsulated into the hydrogels and cultured under 1% O_2 . In the control hydrogel PNHAM-PFCO, MSCs experienced extensive death as dsDNA content was continuously decreased during the culture (Fig. 6B). At day 14, the dsDNA content was less than 10% of that at day 1. In contrast, dsDNA content in the hydrogels with PFC was increased during the 14-day culture period (Fig. 6B). The dsDNA content at day 14 was 2.4 times and 3.6 times of that at day 1 for PNHAM-PFC5 and PNHAM-PFC10 hydrogels respectively (p < 0.01,

day 14 vs. day 1 for both hydrogels). These results show that the PFC-containing, high oxygen preservation hydrogels were able to promote MSC survival under hypoxic condition.

MSC paracrine effects in the hydrogels PNHAM-PFC5 and PNHAM-PFC10 were evaluated in terms of expressions of angiogenic growth factor PDGFB and prosurvival growth factor IGF-1. Real time RT-PCR results showed that PDGFB and IGF-1 expressions were significantly augmented during the 14-day culture period (Fig. 6C and D. p < 0.01 day 14 vs. day 7; p < 0.05 day 7 vs. day 1 for each hydrogel). The above cell paracrine effects and survival results demonstrate that the PFC-containing hydrogels were able to not only promote MSC survival but also modulate their paracrine effects under hypoxic condition.

3.6. In vitro oxygen tension measurements in hydrogels with and without MSCs

A fiber-optic oxygen micro-sensor was used to test the oxygen concentration within the hydrogels under 1% $\rm O_2$ condition. After gelation under atmospheric condition (21% $\rm O_2$) for 30 min, the PNHAM-PFC10, PNHAM-PFC5, PNHAM-PFC0, and DPBS exhibited similar oxygen concentrations as those measured by EPR (Fig. 6F and Table 3). The oxygen concentration gradually decreased after incubation under 1% $\rm O_2$ condition (Fig. 6F). At 168 h, the PNHAM-PFC5 and PNHAM-PFC10 hydrogels exhibited significantly higher oxygen concentrations than the PNHAM-PFC0 hydrogel (p <0.0001).

When MSCs were encapsulated in these 3 hydrogels and incubated under 1% O_2 condition, the oxygen concentrations in the hydrogels also decreased over time. The degree of decrease was greater than that in the hydrogels without MSCs. At 168 h, the oxygen concentrations were 21.1, 59.8, and 63.9 mmHg for PNHAM-PFC0, PNHAM-PFC5, and PNHAM-PFC10 encapsulated with MSCs, respectively (Fig. 6G). These concentrations were lower than those without MSCs at 168 h (28.2 mmHg for PNHAM-PFC0, 67.2 mmHg for PNHAM-PFC5, and 69.9 mmHg for PNHAM-PFC10). The greater

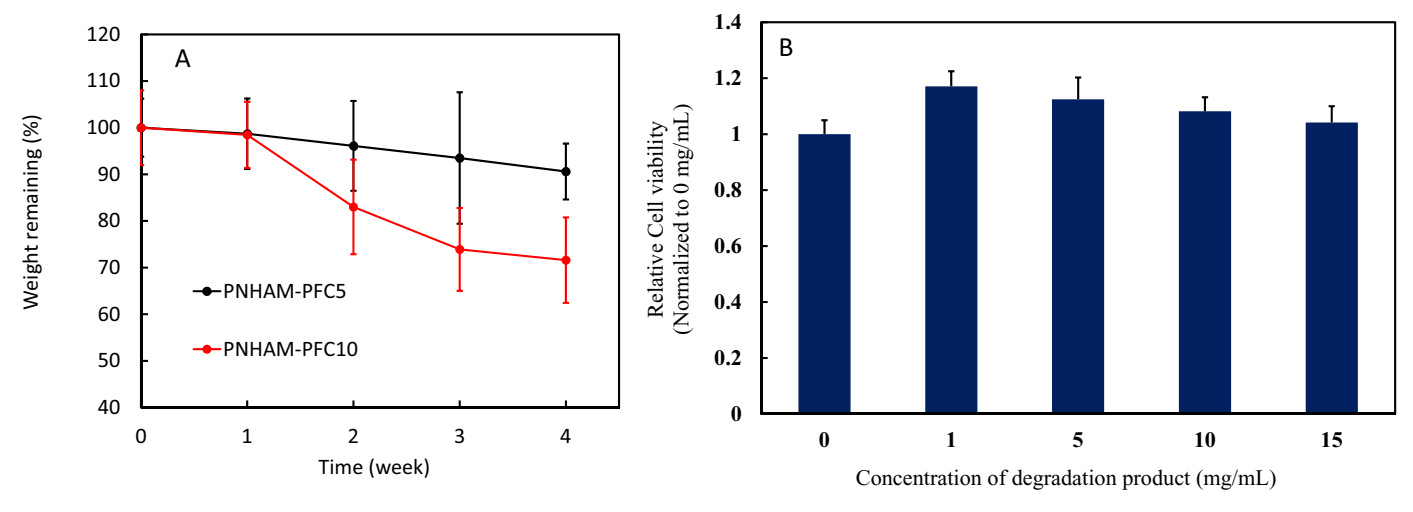


Fig. 5. (A) Degradation of the PNHAM-PFC hydrogels in DPBS at 37 °C for 4 weeks. PNHAM-PFC5 and PNHAM-PFC10 represent hydrogels with PFC content of 5% and 10%, respectively; (B) Cell viability of MSCs cultured in the medium supplemented with final degradation product. The concentration ranged from 0 mg/mL to 15 mg/mL. MTT assay was used to quantify cell viability. The cell viability was normalized to the group without adding final degradation product.

oxygen concentration decrease after MSC encapsulation is likely due to consumption of oxygen by the cells.

3.7. In vivo biocompatibility of the hydrogels

To test hydrogel *in vivo* biocompatibility, PNHAM-PFC5 and PNHAM-PFC10 were implanted subcutaneously in mice for 4 weeks. Collagen gel was employed as a control. F4/80 staining was used to characterize macrophages in the explanted tissues (Fig. 7A). All 3 groups did not experience substantial inflammation (Fig. 7A), and their macrophage ratio was similar to that of the collagen group (Fig. 7B), suggesting that the hydrogels possessed excellent biocompatibility.

4. Discussion

Cell transplantation has been explored extensively for ischemic tissue regeneration. Yet it remains impractical for comprehensive clinical applications due to inferior cell survival under low oxygen condition of the damaged tissues [67]. Various reports have shown that over 98% of the transplanted cells were dead after only two weeks of implantation [59,60,68,69]. To address the issue of oxygen supply after cell transplantation, we have developed high oxygen preservation hydrogels as cell carriers. The oxygen preserved in the hydrogels is able to support cell survival under hypoxic conditions. The developed hydrogels also feature other attractive properties such as fast gelation and thermosensitivity. Fast gelation enables the hydrogels injected into tissues to quickly immobilize with a high cell retention rate [54–58]. Thermosensitivity allows the hydrogels to solidify simply by raising the temperature to body temperature.

The hydrogels were based on NIPAAm, HEMA, AOLA, and MAPEGPFC. NIPAAm was served as a thermosensitive component. HEMA was used to increase hydrophilicity of the hydrogels so as to improve their solubility in aqueous condition at temperatures below their thermal transition temperatures. AOLA component was responsible for hydrogel degradation. PFC was employed to improve oxygen preservation in the hydrogels. The synthesized PFC-containing hydrogels were soluble in DPBS at 4 °C (Fig. 3B). The solutions were readily injectable through 26 G needles. The 4 °C hydrogel solutions were able to quickly solidify within 6 s at 37 °C. The thermal transition temperatures of the hydrogels were dependent on the ratio of MAPEGPFC. The increase in the ratio

augmented the thermal transition temperature (Table 4). This increase is likely due to the increase of hydrogel hydrophilicity as the MAPEGPFC was hydrophilic. This is consistent with water content results where PNHAM-PFC10 exhibited greater water content than PNHAM-PFC5 (Table 4). These results are also consistent with previous reports where the increase of hydrophilic component ratio in PNIPAAm-based hydrogels led to a higher thermal transition temperature and water content [59,70].

The developed hydrogels were soft and flexible at 37 °C (Figs. 3 and 4). Their Young's moduli were in the range of 12 kPa and 18 kPa (Table 4). These moduli were similar to that of the heart muscle [71]. Therefore, the hydrogels are suitable for heart injection as they have potential to effectively decrease elevated wall stress in the left ventricle after myocardial infarction, leading to the increase of cardiac function [9]. The hydrogel modulus was dependent on the MAPEGPFC content. The increase of MAPEGPFC ratio from 5% to 10% decreased Young's modulus. This is expected as the hydrogel water content increase often results in decreased modulus [59,69].

The hydrogels were designed to be degradable by hydrolysis of oligolactide in the side chain. During the 4-week incubation period, the PNHAM-PFC5 and PNHAM-PFC10 gradually lost weight (Fig. 5A). Both hydrogels exhibited similar weight loss during the first week of degradation. The faster degradation was observed for PNHAM-PFC10 beyond 1 week. At week 4, PNHAM-PFC10 had significantly greater weight loss than PNHAM-PFC5. The discrepancy in degradation rate is consistent with hydrogel water content. A greater water content can facilitate hydrolysis of oligolactide in the hydrogels leading to increased weight loss. To determine thermal properties of the final degradation product, the polymer with the same composition as PNHAM-PFC10 after complete degradation of oligolactide was synthesized. The final degradation product had a thermal transition temperature 48.5 °C. As this temperature is above 37 °C, the final degradation products cannot solidify but dissolve in the body fluid. The increase of thermal transition temperature is due to conversion of hydrophobic AOLA units into hydrophilic acrylic acid units after hydrolysis. We found in our previous report that increase of hydrophilicity of the PNIPAAmbased hydrogels can elevate their thermal transition temperatures [54-58].

The final degradation product was biocompatible as it did not decrease fibroblast viability even when the concentration was as high as 15 mg/mL (Fig. 5B). Hydrogel *in vitro* biocompatibility before degradation was tested in terms of its capability to support

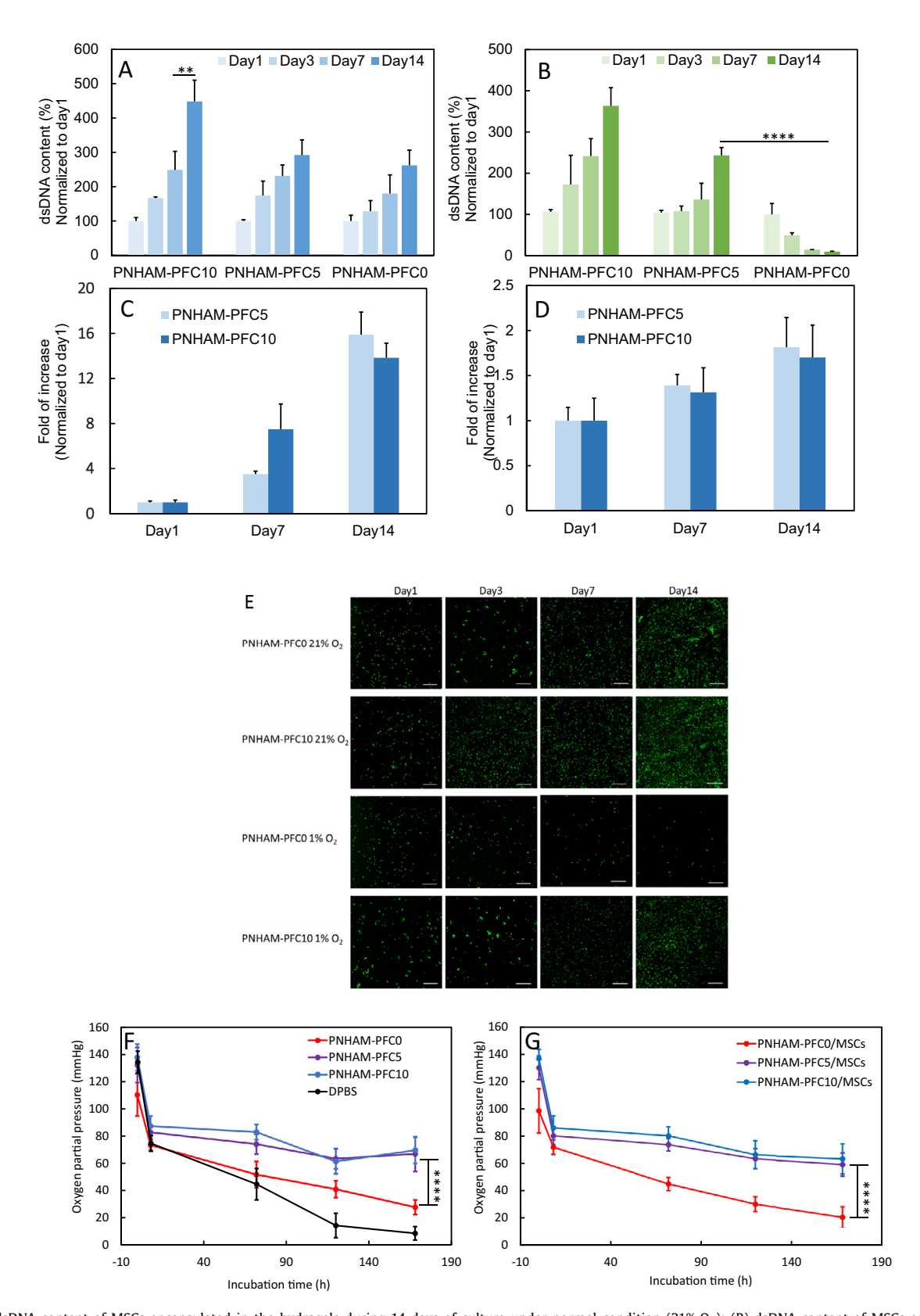


Fig. 6. (A) dsDNA content of MSCs encapsulated in the hydrogels during 14 days of culture under normal condition $(21\% \ O_2)$; (B) dsDNA content of MSCs encapsulated in the hydrogels during 14 days of culture under hypoxic condition $(1\% \ O_2)$; Gene expressions of (C) PDGFB and (D) IGF-1 were determined by real time RT-PCR; (E) Live cell images of MSCs encapsulated in two hydrogels, PNHHAM-PFC0 and PNHAM-PFC10, under 21% and 1% O_2 during 14 days of culture period. Scale bar = 200 μ m; (F) Oxygen partial pressure within hydrogels at 0 h, 8 h, 72 h, 120 h and 168 h; (G) Oxygen tension within cell-encapsulated hydrogels at 0 h, 8 h, 72 h, 120 h and 168 h (n = 7; **: p < 0.001; ***: p < 0.001). DPBS was used as a control. PNHAM-PFC0, PNHAM-PFC10 represent hydrogels without PFC conjugation, with PFC content of 5% and 10%, respectively.

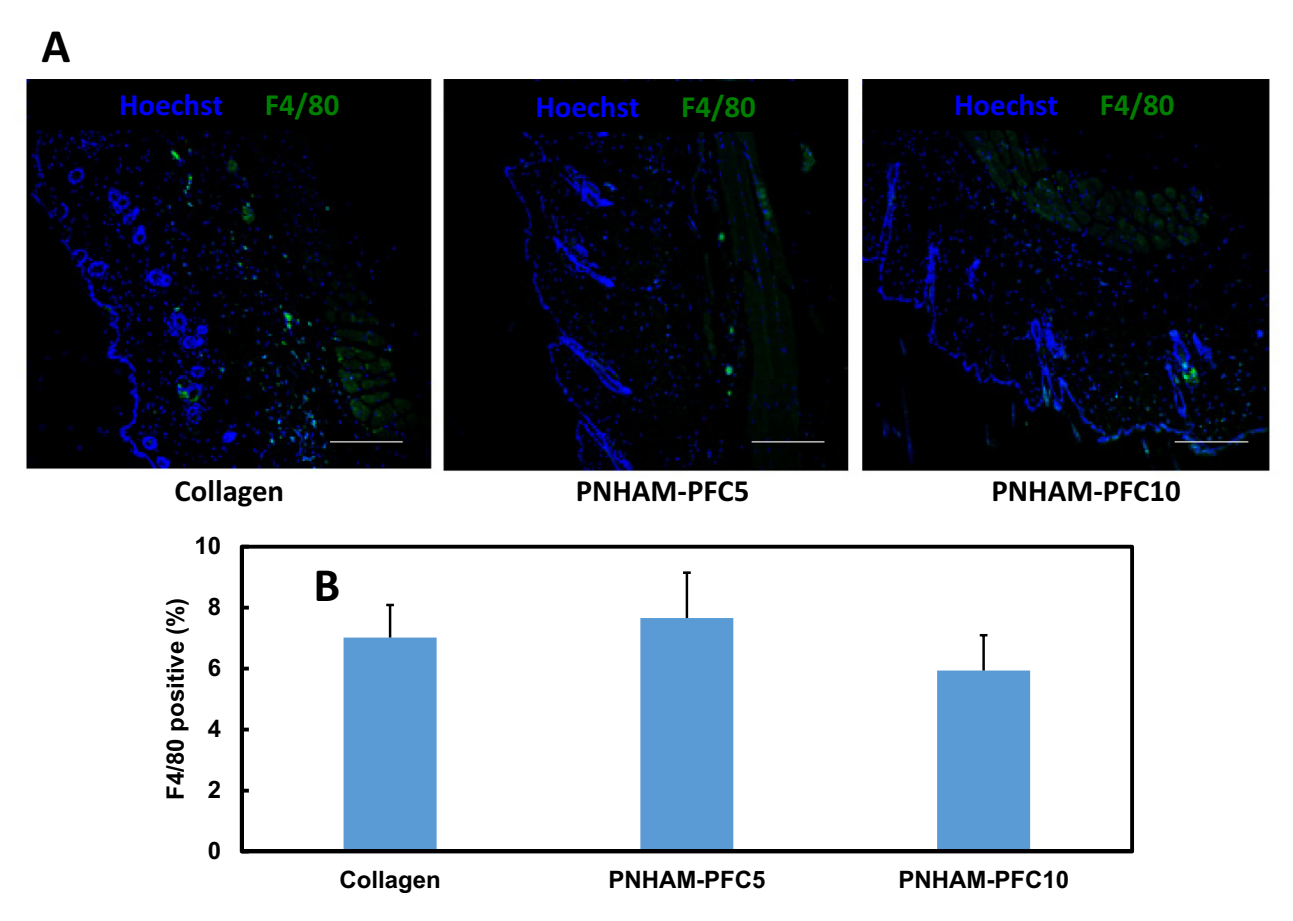


Fig. 7. Subcutaneous implantation of hydrogels in C57BL/6 mice. (A) F4/80 immunofluorescent staining of tissues after subcutaneous implantation for 4 weeks; and (B)) ratio of F4/80 positive cells in tissues. The mice without injection were used as control. PNHAM-PFC5 and PNHAM-PFC10 represent hydrogels with PFC content of 5% and 10%, respectively. Scale bar = $50 \mu m$.

MSC survival and proliferation under normal culture conditions (21% O₂). MSCs were able to grow inside the hydrogels during a 2-week culture period (Fig. 6A and B). To determine *in vivo* biocompatibility of the hydrogels, they were injected subcutaneously into mice. The collagen gel that has excellent biocompatibility was used as control. After 4 weeks, the tissues injected with the PNHAM-PFC5 and PNHAM-PFC10 hydrogels did not show substantial inflammatory reaction compared with control collagen hydrogel (Fig. 7A). F4/80 staining results demonstrate that macrophage recruitment of PNHAM-PFC5 and PNHAM-PFC10 hydrogels was as low as collagen hydrogel (Fig. 7B). Overall, the developed hydrogels exhibited excellent biocompatibility *in vitro* and *in vivo*.

The oxygen preservation property of the hydrogels was characterized by EPR in terms of pO_2 under hypoxic condition (1% O_2) after the hydrogels were transferred from normal condition (21% O_2). The pO_2 of the hydrogel without PFC was much lower than that of the DPBS in the normal condition. The pO_2 was increased to that of DPBS after 5% PFC was introduced into the hydrogel. When the PFC content was increased to 10%, the pO_2 was even greater than that of DPBS (Table 3). These results demonstrate that introduction of PFC into hydrogels facilitated oxygen binding, leading to an augmentation of oxygen preservation.

Ischemic tissues are characterized by a low oxygen content that hinders the survival of transplanted cells [69,72,73]. While cells may be tolerant of an oxygen level ~5% [74], they experience significant death when the oxygen level drops to 1%, a condition similar to that in the ischemic tissues [75,76]. When MSCs were encapsulated in hydrogel with a low oxygen preservation capability (PNHAM-PFCO), more than 90% of the cells were dead after 14 days

of culture under 1% O₂ (Fig. 6B). In contrast, MSCs encapsulated in the hydrogels with high oxygen preservation capability (PNHAM-PFC5 and PNHAM-PFC10) did not experience death, rather, MSCs proliferated under the same low oxygen condition (Fig. 6B). In addition, hydrogel with a higher pO2 more significantly promoted MSC proliferation (PNHAM-PFC5 vs. PNHAM-PFC10). It is possible that the cells consumed the oxygen preserved in the hydrogels, and facilitated their survival and proliferation. The above results demonstrate that hydrogels with high oxygen preservation capability can potentially be used to deliver cells into ischemic tissues for improved cell survival. These results are consistent with previous reports where controlled release of molecular oxygen improved cell survival under hypoxic conditions [9,10]. The duration of the developed hydrogels in promoting cell survival is longer than those reported PFC-conjugated chitosan hydrogels. In this study, we found that PNHAM-PFC5 and PNHAM-PFC10 enhanced MSC survival under hypoxic condition for 14 days. In contrast, the PFC-conjugated chitosan hydrogels promoted neural stem cell survival under normal oxygen condition for 8 days [77].

To understand the mechanism of the developed oxygen preservation hydrogels in promoting MSC survival, oxygen tension in the hydrogels with and without MSCs were monitored under 1% O2 condition for 7 days (Fig. 6F and G). In the hydrogels without MSCs, the oxygen tension for PNHAM-PFCO was decreased to 28.2 mmHg at day 7, while it maintained above 61.7 mmHg in the two PFC-conjugated hydrogels during the entire testing period (Fig. 6F). After encapsulation of MSCs, the oxygen tension in all 3 hydrogels was decreased compared to that in the corresponding hydrogels without MSCs (Fig. 6G), likely attributed to the oxygen

consumption by the cells. Yet the oxygen tension in the PNHAM-PFC5 and PNHAM-PFC10 hydrogels kept greater than PNHAM-PFC0 during 7 days. The remaining oxygen in the hydrogels promoted cell survival beyond 7 days (Fig. 6B). In our future studies, we will deliver MSCs using the developed hydrogels into ischemic tissues such as ischemic limb and infarcted cardiac muscle to systematically test the efficacy of these hydrogels in improving MSC survival, leading to tissue repair and functional improvement.

5. Conclusions

A family of PFC-containing, high oxygen preservation hydrogels have been developed to improve cell survival under hypoxia. The hydrogels were also fast gelling, thermosensitive, injectable, and degradable. Under 1% $\rm O_2$, the hydrogels possessed a greater $\rm pO_2$ than DPBS. The high oxygen preservation hydrogels promoted MSC survival and proliferation under hypoxic conditions but the cells experienced extensive death in low oxygen preservation hydrogels. These high oxygen preservation hydrogels are attractive for cell therapy involving regeneration of ischemic tissues.

Declaration of Competing Interest

The authors declare that they have no known competing financial interests or personal relationships that could have appeared to influence the work reported in this paper.

Acknowledgments

The authors thank Dr. Jonathan Barnes and Dr. Xuesong Li in the Department of Chemistry at the Washington University in St Louis for help on molecular weight measurements. This work was supported by US National Institutes of Health (R01HL138175, R01HL138353, R01EB022018, R01AG056919, and R21EB021896), and National Science Foundation (1708956).

References

- [1] T. Giri, A. Alexander, M. Agrawal, S. Saraf, Current status of stem cell therapies in tissue repair and regeneration, Curr. Stem Cell Res. Ther. (2018).
- [2] X. Li, K. Tamama, X. Xie, J. Guan, Improving cell engraftment in cardiac stem cell therapy, Stem Cells Int. 2016 (2016).
- [3] H.Y. Kim, S.Y. Kim, H.-Y. Lee, J.H. Lee, G.-J. Rho, H.-J. Lee, H.-C. Lee, J.-H. Byun, S.H. Oh, Oxygen-Releasing microparticles for cell survival and differentiation ability under hypoxia for effective bone regeneration, Biomacromolecules (2019).
- [4] X. Sun, H. Zhang, J. He, R. Cheng, Y. Cao, K. Che, L. Cheng, L. Zhang, G. Pan, P. Ni, Adjustable hardness of hydrogel for promoting vascularization and maintaining stemness of stem cells in skin flap regeneration, Appl. Mater. Today 13 (2018) 54–63.
- [5] R.J. Henning, Therapeutic angiogenesis: angiogenic growth factors for ischemic heart disease, Future Cardiol. 12 (5) (2016) 585–599.
- [6] X.L. Aranguren, C.M. Verfaillie, A. Luttun, Emerging hurdles in stem cell therapy for peripheral vascular disease, J. Mol. Med. 87 (1) (2009) 3–16.
- [7] A.Y. Cheng, A.J. García, Engineering the matrix microenvironment for cell delivery and engraftment for tissue repair, Curr. Opin. Biotechnol. 24 (5) (2013) 864–871.
- [8] Y. Li, W. Liu, F. Liu, Y. Zeng, S. Zuo, S. Feng, C. Qi, B. Wang, X. Yan, A. Khademhosseini, Primed 3D injectable microniches enabling low-dosage cell therapy for critical limb ischemia, Proc. Natl. Acad. Sci. 111 (37) (2014) 13511–13516.
- [9] Z. Fan, Z. Xu, H. Niu, N. Gao, Y. Guan, C. Li, Y. Dang, X. Cui, X.L. Liu, Y. Duan, An injectable oxygen release system to augment cell survival and promote cardiac repair following myocardial infarction, Sci. Rep. 8 (1) (2018) 1371.
- [10] Z. Li, X. Guo, J. Guan, An oxygen release system to augment cardiac progenitor cell survival and differentiation under hypoxic condition, Biomaterials 33 (25) (2012) 5914–5923.
- [11] S. Daly, M. Thorpe, S. Rockswold, M. Hubbard, T. Bergman, U. Samadani, G. Rockswold, Hyperbaric oxygen therapy in the treatment of acute severe traumatic brain injury: a systematic review, J. Neurotrauma 35 (4) (2018) 623–629.
- [12] G. Almosnino, J.R. Holm, S.R. Schwartz, D.M. Zeitler, The role of hyperbaric oxygen as salvage therapy for sudden sensorineural hearing loss, Ann. Otol. Rhinol. Laryngol. 127 (10) (2018) 672–676.

- [13] J. Liao, M.-J. Wu, Y.-D. Mu, P. Li, J. Go, Impact of hyperbaric oxygen on tissue healing around dental implants in beagles, Med. Sci. Moni. Int. Med. J. Experim. Clini. Res. 24 (2018) 8150.
- [14] M.M. Coronel, R. Geusz, C.L. Stabler, Mitigating hypoxic stress on pancreatic islets via in situ oxygen generating biomaterial, Biomaterials 129 (2017) 139–151.
- [15] Z. Ahmed, E.A. Gooding, K.V. Pimenov, L. Wang, S.A. Asher, UV resonance Raman determination of molecular mechanism of poly (N-isopropylacrylamide) volume phase transition, J. Phys. Chem. B 113 (13) (2009) 4248–4256.
- [16] M.M. Sthijns, C.A. van Blitterswijk, V.L. LaPointe, Redox regulation in regenerative medicine and tissue engineering: the paradox of oxygen, J. Tissue Eng. Regen. Med. 12 (10) (2018) 2013–2020.
- [17] A. Maio, R. Scaffaro, L. Lentini, A.P. Piccionello, I. Pibiri, Perfluorocarbons graphene oxide nanoplatforms as biocompatible oxygen reservoirs, Chem. Eng. I. 334 (2018) 54–65.
- [18] H.Y. Kim, S.Y. Kim, H.Y. Lee, J.H. Lee, G.J. Rho, H.J. Lee, H.C. Lee, J.H. Byun, S.H. Oh, Oxygen-Releasing microparticles for cell survival and differentiation ability under hypoxia for effective bone regeneration, Biomacromolecules 20 (2) (2019) 1087–1097.
- [19] B. Pandya, A. Sheikh, J. Spagnola, S. Bekheit, J. Lafferty, M. Kowalski, Safety and efficacy of second-generation versus first-generation cryoballoons for treatment of atrial fibrillation: a meta-analysis of current evidence, J. Intervent. Cardiac Electrophysiol. 45 (1) (2016) 49–56.
- [20] L. Wei, J. Wang, Y. Cao, Q. Ren, L. Zhao, X. Li, J. Wang, Hyperbaric oxygenation promotes neural stem cell proliferation and protects the learning and memory ability in neonatal hypoxic-ischemic brain damage, Int. J. Clin Exp. Pathol. 8 (2) (2015) 1752–1759.
- [21] M. Dhar, N. Neilsen, K. Beatty, S. Eaker, H. Adair, D. Geiser, Equine peripheral blood-derived mesenchymal stem cells: isolation, identification, trilineage differentiation and effect of hyperbaric oxygen treatment, Equine Vet. J. 44 (5) (2012) 600–605.
- [22] M. Khan, S. Meduru, R. Gogna, E. Madan, L. Citro, M.L. Kuppusamy, M. Sayyid, M. Mostafa, R.L. Hamlin, P. Kuppusamy, Oxygen cycling in conjunction with stem cell transplantation induces NOS3 expression leading to attenuation of fibrosis and improved cardiac function, Cardiovasc. Res. 93 (1) (2012) 89–99.
- [23] N. Hampson, D. Atik, Central Nervous System Oxygen Toxicity During Routine Hyperbaric Oxygen Therapy (2003).
- [24] B.S. Harrison, D. Eberli, S.J. Lee, A. Atala, J.J. Yoo, Oxygen producing biomaterials for tissue regeneration, Biomaterials 28 (31) (2007) 4628–4634.
- [25] S.H. Oh, C.L. Ward, A. Atala, J.J. Yoo, B.S. Harrison, Oxygen generating scaffolds for enhancing engineered tissue survival, Biomaterials 30 (5) (2009) 757–762.
- [26] E. Pedraza, M.M. Coronel, C.A. Fraker, C. Ricordi, C.L. Stabler, Preventing hypoxia-induced cell death in beta cells and islets via hydrolytically activated, oxygen-generating biomaterials, Proc. Natl. Acad. Sci. U.S.A. 109 (11) (2012) 4245–4250
- [27] S. Park, K.M. Park, Hyperbaric oxygen-generating hydrogels, Biomaterials 182 (2018) 234–244.
- [28] S.M. Ng, J.Y. Choi, H.S. Han, J.S. Huh, J.O. Lim, Novel microencapsulation of potential drugs with low molecular weight and high hydrophilicity: hydrogen peroxide as a candidate compound, Int. J. Pharm. 384 (1–2) (2010) 120–127.
- [29] S.E. Bae, J.S. Son, K. Park, D.K. Han, Fabrication of covered porous PLGA microspheres using hydrogen peroxide for controlled drug delivery and regenerative medicine, J. controll. release offic. j. Controll. Release Soc. 133 (1) (2009) 37-43.
- [30] R. Lin, H. Chen, D. Callow, S. Li, L. Wang, S. Li, L. Chen, J. Ding, W. Gao, H. Xu, Multifaceted effects of astragaloside iv on promotion of random pattern skin flap survival in rats, Am. J. Transl. Res. 9 (9) (2017) 4161.
- [31] S. Bhattacharya, Reactive oxygen species and cellular defense system, in: Free Radicals in Human Health and Disease, Springer, 2015, pp. 17–29.
- [32] J. Tan, D. Liu, Y. Bai, C. Huang, X. Li, J. He, Q. Xu, L. Zhang, Enzyme-as-sisted photoinitiated polymerization-induced self-assembly: an oxygen-toler-ant method for preparing block copolymer nano-objects in open vessels and multiwell plates, Macromolecules 50 (15) (2017) 5798–5806.
- [33] Q. Chen, J. Chen, C. Liang, L. Feng, Z. Dong, X. Song, G. Song, Z. Liu, Drug-induced co-assembly of albumin/catalase as smart nano-theranostics for deep intra-tumoral penetration, hypoxia relieve, and synergistic combination therapy, J. Controll. Release 263 (2017) 79–89.
- [34] Z. Li, X. Guo, J. Guan, An oxygen release system to augment cardiac progenitor cell survival and differentiation under hypoxic condition, Biomaterials 33 (25) (2012) 5914–5923.
- [35] N. Alemdar, J. Leijten, G. Camci-Unal, J. Hjortnaes, J. Ribas, A. Paul, P. Mostafalu, A.K. Gaharwar, Y. Qiu, S. Sonkusale, Oxygen-generating photo-cross-linkable hydrogels support cardiac progenitor cell survival by reducing hypoxia-induced necrosis, ACS Biomater. Sci. Eng. 3 (9) (2016) 1964–1971.
- [36] J.M. García-Ruiz, C. Galán-Arriola, R. Fernández-Jiménez, J. Aguero, J. Sánchez-González, A. García-Alvarez, M. Nuno-Ayala, G.P. Dubé, Z. Zafirelis, G.J. López-Martín, Bloodless reperfusion with the oxygen carrier HBOC-201 in acute myocardial infarction: a novel platform for cardioprotective probes delivery, Basic Res. Cardiol. 112 (2) (2017) 17.
- [37] N.P. Lee, K.T. Chan, M.Y. Choi, H.Y. Lam, L.N. Tung, F.C. Tzang, H. Han, I.P. Lam, S.Y. Kwok, S.H. Lau, Oxygen carrier YQ23 can enhance the chemotherapeutic drug responses of chemoresistant esophageal tumor xenografts, Cancer Chemother. Pharmacol. 76 (6) (2015) 1199–1207.
- [38] P.E. Keipert, in: Hemoglobin-based Oxygen Carrier (HBOC) Development in

- trauma: Previous Regulatory challenges, Lessons learned, and a Path forward, Oxygen Transport to Tissue XXXIX, Springer, 2017, pp. 343–350.
- [39] C.-C. Huang, W.-T. Chia, M.-F. Chung, K.-J. Lin, C.-W. Hsiao, C. Jin, W.-H. Lim, C.-C. Chen, H.-W. Sung, An implantable depot that can generate oxygen in situ for overcoming hypoxia-induced resistance to anticancer drugs in chemotherapy, J. Am. Chem. Soc. 138 (16) (2016) 5222–5225.
- [40] K. Chin, S.F. Khattak, S.R. Bhatia, S.C. Roberts, Hydrogel-perfluorocarbon composite scaffold promotes oxygen transport to immobilized cells, Biotechnol. Prog. 24 (2) (2008) 358–366.
- [41] J.C. White, W.L. Stoppel, S.C. Roberts, S.R. Bhatia, Addition of perfluorocarbons to alginate hydrogels significantly impacts molecular transport and fracture stress, J Biomed Mater Res A 101 (2) (2013) 438–446.
- [42] D.G. Seifu, T.T. Isimjan, K. Mequanint, Tissue engineering scaffolds containing embedded fluorinated-zeolite oxygen vectors, Acta Biomater 7 (10) (2011) 3670–3678
- [43] F. Le Pape, L. Cosnuau-Kemmat, G. Richard, F. Dubrana, C. Ferec, F. Zal, E. Leize, P. Delepine, HEMOXCell, a new oxygen carrier usable as an additive for mesenchymal stem cell culture in platelet lysate-supplemented media, Artif Organs 41 (4) (2017) 359–371.
- [44] H. Newland, D. Eigel, A.E. Rosser, C. Werner, B. Newland, Oxygen producing microscale spheres affect cell survival in conditions of oxygen-glucose deprivation in a cell specific manner: implications for cell transplantation, Biomater Sci 6 (10) (2018) 2571–2577.
- [45] A.I. Alayash, Blood substitutes: why haven't we been more successful? Trends Biotechnol. 32 (4) (2014) 177–185.
- [46] Z. Tao, P.P. Ghoroghchian, Microparticle, nanoparticle, and stem cell-based oxygen carriers as advanced blood substitutes, Trends Biotechnol. 32 (9) (2014) 466–473.
- [47] G. Takeshi, M. Gaku, K. Ken-Ichi, A novel column fermentor having a wetted-wall of perfluorocarbon as an oxygen carrier, Biochem. Eng. J. 8 (2) (2001) 165–169
- [48] J.P. Sullivan, J.E. Gordon, A.F. Palmer, Simulation of oxygen carrier mediated oxygen transport to C3A hepatoma cells housed within a hollow fiber bioreactor, Biotechnol. Bioeng. 93 (2) (2006) 306–317.
- [49] B.D. Spiess, R. Cochran, Perfluorocarbon emulsions and cardiopulmonary bypass: a technique for the future, J. Cardiothorac. Vasc. Anesth. 10 (1) (1996) 83–90
- [50] H. Lawall, P. Bramlage, B. Amann, Stem cell and progenitor cell therapy in peripheral artery disease, Thromb. Haemost. 103 (04) (2010) 696–709.
- [51] M. Gholipourmalekabadi, S. Zhao, B.S. Harrison, M. Mozafari, A.M. Seifalian, Oxygen-generating biomaterials: a new, viable paradigm for tissue engineering? Trends Biotechnol. 34 (12) (2016) 1010–1021.
- [52] J.G. Riess, Understanding the fundamentals of perfluorocarbons and perfluorocarbon emulsions relevant to in vivo oxygen delivery, Artific. Cells, Blood Subst. Biotechnol. 33 (1) (2005) 47–63.
- [53] A.L. Farris, A.N. Rindone, W.L. Grayson, Oxygen delivering biomaterials for tissue engineering, J. Mat. Chem. B 4 (20) (2016) 3422–3432.
- [54] Z. Fan, Z. Xu, H. Niu, N. Gao, Y. Guan, C. Li, Y. Dang, X. Cui, X.L. Liu, Y. Duan, H. Li, X. Zhou, P.H. Lin, J. Ma, J. Guan, An injectable oxygen release system to augment cell survival and promote cardiac repair following myocardial infarction, Sci. Rep. 8 (1) (2018) 1371.
- [55] Z. Fan, Z. Xu, H. Niu, Y. Sui, H. Li, J. Ma, J. Guan, Spatiotemporal delivery of basic fibroblast growth factor to directly and simultaneously attenuate cardiac fibrosis and promote cardiac tissue vascularization following myocardial infarction, J. Controlled Release offic. j. Controll. Rel. Soc. 311-312 (2019) 233-244.
- [56] C. Li, Z. Huang, N. Gao, J. Zheng, J. Guan, Injectable, thermosensitive, fast gelation, bioeliminable, and oxygen sensitive hydrogels, materials science & engineering. c, Mater. Biolog. Appl. 99 (2019) 1191–1198.
- [57] Z. Li, Z. Fan, Y. Xu, W. Lo, X. Wang, H. Niu, X. Li, X. Xie, M. Khan, J. Guan, pH-Sensitive and thermosensitive hydrogels as stem-cell carriers for cardiac therapy, ACS Appl. Mater Interfaces 8 (17) (2016) 10752–10760.

- [58] L. Teng, Y. Chen, Y.G. Jia, L. Ren, Supramolecular and dynamic covalent hydrogel scaffolds: from gelation chemistry to enhanced cell retention and cartilage regeneration, J. Mater. Chem. B 7 (43) (2019) 6705–6736.
- [59] H. Niu, X. Li, H. Li, Z. Fan, J. Ma, J. Guan, Thermosensitive, fast gelling, photoluminescent, highly flexible, and degradable hydrogels for stem cell delivery, Acta Biomater 83 (2019) 96–108.
- [60] F. Wang, Z. Li, M. Khan, K. Tamama, P. Kuppusamy, W.R. Wagner, C.K. Sen, J. Guan, Injectable, rapid gelling and highly flexible hydrogel composites as growth factor and cell carriers, Acta Biomater 6 (6) (2010) 1978–1991.
- [61] M. Dinguizli, S. Jeumont, N. Beghein, J. He, T. Walczak, P. Lesniewski, H. Hou, O. Grinberg, A. Sucheta, H. Swartz, Development and evaluation of biocompatible films of polytetrafluoroethylene polymers holding lithium phthalocyanine crystals for their use in EPR oximetry, Biosensors Bioelectron. 21 (7) (2006) 1015–1022.
- [62] H. Feil, Y.H. Bae, J. Feijen, S.W. Kim, Effect of comonomer hydrophilicity and ionization on the lower critical solution temperature of N-isopropylacrylamide copolymers, Macromolecules 26 (10) (1993) 2496–2500.
- [63] Z. Fan, M. Fu, Z. Xu, B. Zhang, Z. Li, H. Li, X. Zhou, X. Liu, Y. Duan, P.-H. Lin, Sustained release of a peptide-based matrix metalloproteinase-2 inhibitor to attenuate adverse cardiac remodeling and improve cardiac function following myocardial infarction, Biomacromolecules (2017).
- [64] Y. Xu, M. Fu, Z. Li, Z. Fan, X. Li, Y. Liu, P.M. Anderson, X. Xie, Z. Liu, J. Guan, A prosurvival and proangiogenic stem cell delivery system to promote ischemic limb regeneration, Acta Biomater 31 (2016) 99–113.
- [65] Y. Xu, M. Fu, Z. Li, Z. Fan, X. Li, Y. Liu, P.M. Anderson, X. Xie, Z. Liu, J. Guan, A prosurvival and proangiogenic stem cell delivery system to promote ischemic limb regeneration, Acta Biomater 31 (2016) 99–113.
- [66] C.N. Lumeng, J.L. Bodzin, A.R. Saltiel, Obesity induces a phenotypic switch in adipose tissue macrophage polarization, J. Clin. Invest. 117 (1) (2007) 175–184.
- [67] S. Lee, E. Choi, M.-J. Cha, K.-C. Hwang, Cell adhesion and long-term survival of transplanted mesenchymal stem cells: a prerequisite for cell therapy, Oxid. Med. Cell Longev 2015 (2015).
- [68] T. Reffelmann, R.A. Kloner, Cellular cardiomyoplasty—cardiomyocytes, skeletal myoblasts, or stem cells for regenerating myocardium and treatment of heart failure? Cardiovasc. Res. 58 (2) (2003) 358–368.
- [69] Z. Li, X. Guo, J. Guan, A thermosensitive hydrogel capable of releasing bFGF for enhanced differentiation of mesenchymal stem cell into cardiomyocyte-like cells under ischemic conditions, Biomacromolecules 13 (6) (2012) 1956–1964.
- [70] Z. Li, F. Wang, S. Roy, C.K. Sen, J. Guan, Injectable, highly flexible, and ther-mosensitive hydrogels capable of delivering superoxide dismutase, Biomacro-molecules 10 (12) (2009) 3306–3316.
- [71] J. Ophir, I. Cespedes, B. Garra, H. Ponnekanti, Y. Huang, N. Maklad, Elastog-raphy: ultrasonic imaging of tissue strain and elastic modulus in vivo, Eur. j. ultrasound 3 (1) (1996) 49–70.
- [72] W. Zhu, J. Chen, X. Cong, S. Hu, X. Chen, Hypoxia and serum deprivation-in-duced apoptosis in mesenchymal stem cells, Stem. Cells 24 (2) (2006) 416–425.
- [73] E. Potier, E. Ferreira, A. Meunier, L. Sedel, D. Logeart-Avramoglou, H. Petite, Prolonged hypoxia concomitant with serum deprivation induces massive human mesenchymal stem cell death, Tissue Eng. 13 (6) (2007) 1325–1331.
- [74] D.P. Lennon, J.M. Edmison, A.I. Caplan, Cultivation of rat marrow-derived mesenchymal stem cells in reduced oxygen tension: effects on in vitro and in vivo osteochondrogenesis, J. Cell. Physiol. 187 (3) (2001) 345–355.
- [75] A. Salim, R.P. Nacamuli, E.F. Morgan, A.J. Giaccia, M.T. Longaker, Transient changes in oxygen tension inhibit osteogenic differentiation and runx2 expression in osteoblasts, J. Biol. Chem. 279 (38) (2004) 40007–40016.
- [76] G.Y. Rochefort, B. Delorme, A. Lopez, O. Hérault, P. Bonnet, P. Charbord, V. Eder, J. Domenech, Multipotential mesenchymal stem cells are mobilized into peripheral blood by hypoxia, Stem Cells 24 (10) (2006) 2202–2208.
- [77] H. Li, A. Wijekoon, N.D. Leipzig, Encapsulated neural stem cell neuronal differentiation in fluorinated methacrylamide chitosan hydrogels, Ann. Biomed. Eng. 42 (7) (2014) 1456–1469.